JOURNAL OF MATERIALS SCIENCE 30 (1995) 5931–5938

Functionally graded nickel–aluminide and iron–aluminide coatings produced via laser cladding

J. H. ABBOUD, R. D. RAWLINGS, D. R. F. WEST
Department of Materials, Imperial College of Science and Technology, London SW7 2BP

Functionally graded nickel–aluminide and iron–aluminide in the form of superimposed clad layers up to ~ 4 mm total thickness were produced on nickel and on iron based substrates, respectively. A continuous wave carbon dioxide laser and two separate powder feeders were employed. The processing parameters were: 1.8 kW laser power, 3 mm beam diameter, and 7 mm s^{-1} traverse speed. A series of single clad layers with various Al contents were first produced in order to obtain fundamental data required for the processing of functionally graded materials. Functionally graded Ni–Al and Fe–Al coatings (up to three layers) were produced by successive deposition of clad layers normal to the substrate surface. Compositional control was achieved by keeping the powder flow of Ni or Fe constant and changing the flow rate of Al. Microstructures are interpreted and discussed in relation to aluminides based on the Ni–Al and Fe–Al systems.

1. Introduction

Laser cladding is a technique used to coat a substrate with a layer of other materials to improve surface properties such as resistance to corrosion, erosion or wear. The process typically involves blowing a powder mixture pneumatically into the laser melted zone. The processing parameters such as laser power, traverse speed, and powder flow rate are controlled to achieve the required thickness with minimum dilution from the substrate.

In cases where the clad materials and the substrate have different physical and mechanical properties, the interface may be a potential area of weakness which may lead to failure during service. In such situations it may be advantageous to produce clads which incorporate a gradient of composition and structure. Laser processing offers a potential route to produce functionally graded (FG) coatings. Recent work by the authors has demonstrated that functionally graded titanium–aluminide coated layers with Al contents from 22 at % to 47 at % can be produced on a titanium substrate by successive deposition of three clad layers [1]. Also FG titanium–aluminide composite with increasing Al content can be produced by incorporating ceramic particles with the titanium and aluminium powders [2]. Similarly, Jasim *et al.* [3] showed that by using three powder mixtures, a functionally graded region, with a progressive increase in aluminium and SiC, can be built up on a nickel base alloy by three superimposed clad layers. These previous studies on producing functionally graded material via cladding employed one powder feeder with various premixed powders.

The present report concerns the use of two feeders to produce FG Ni–Al and Fe–Al coated layers on a nickel base alloy and low carbon steel substrate, respectively. The composition of each layer was changed by changing the flow rate of one powder (aluminium) while keeping the others (nickel or iron) constant.

2. Experimental procedure

A 2 kW CW CO_2 laser operated at 1.8 kW laser power and 3 mm beam diameter was used in this investigation. The substrates were either Ni alloy of analysed composition (Ni–26%Cr–6%Mo–11.5% Co–1.5%Fe–1.6%Al, all in at %) or a low carbon steel. The traverse speed was kept constant at 7 mm s^{-1}. The cladding materials (Ni, Fe, and Al) were in the form of powder with particle sizes ranging between 50 and 100 μm. Two separate powder feeders were employed. One for Ni or Fe and the other for Al, and the flow rate was changed by variation of the rotation speed of the screw. Single clad layers of Ni–Al and Fe–Al with various Al contents were produced by changing the Al flow rate while the Ni or Fe powder flow rates and other laser processing parameters were kept constant. Information from this series of single clads was used to select the processing parameters for the production of functionally graded Ni–Al or Fe–Al coatings with increasing Al content by superimposition of several clad layers normal to the surface of the substrate.

Transverse sections were prepared from the single and multiple clad layers for metallographic and

0022–2461

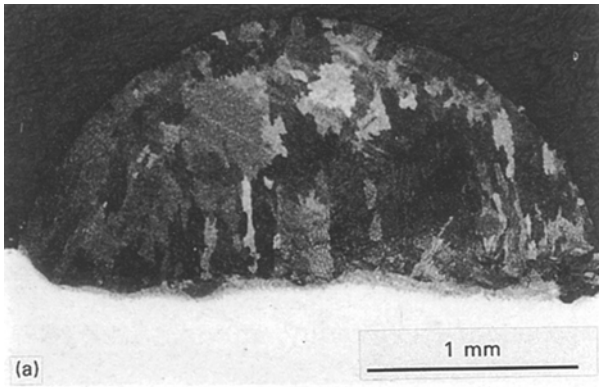

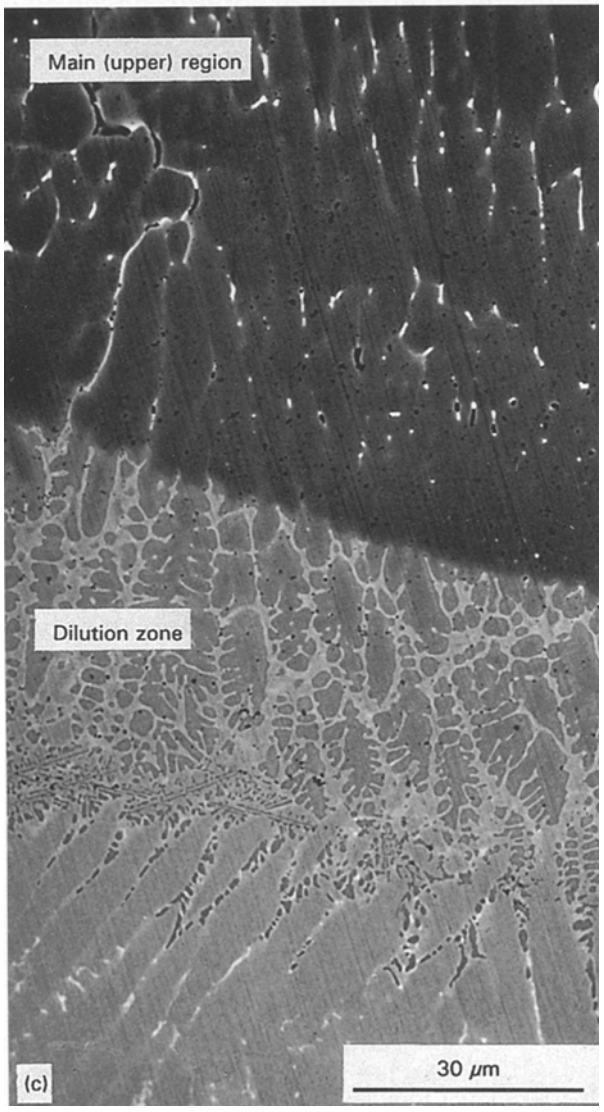

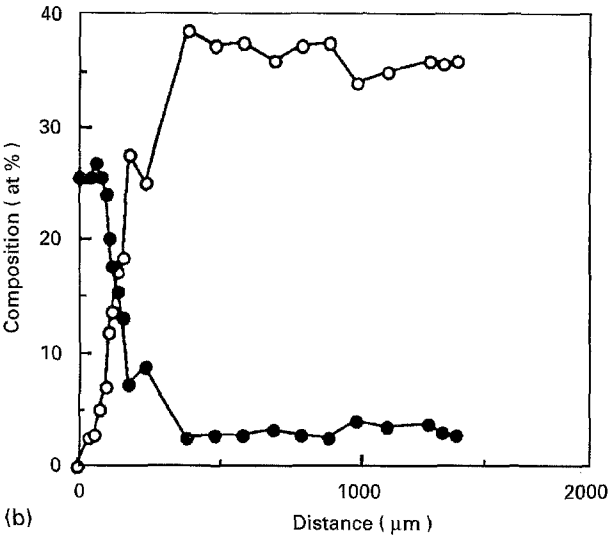

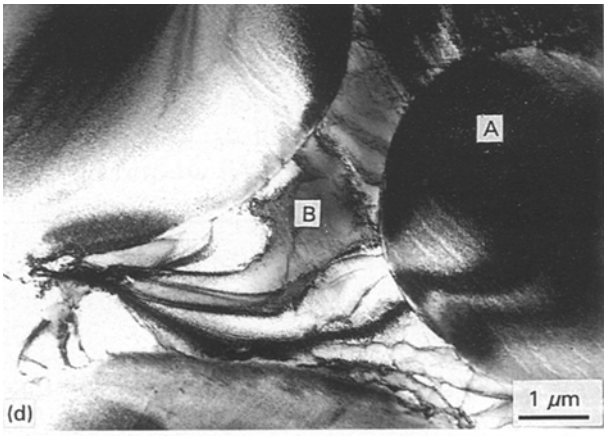

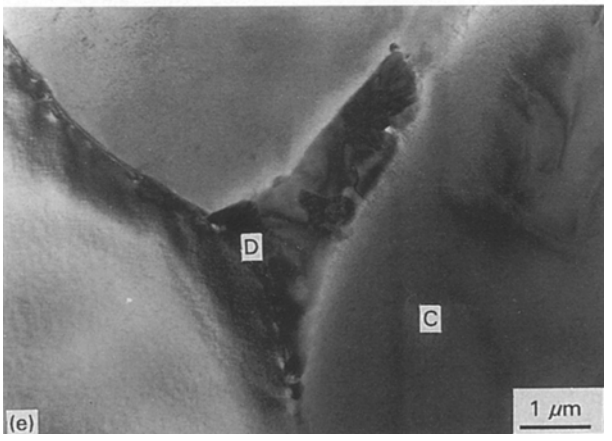

Figure 1 Ni–Al single clad layer produced at 1.8 kW, 3 mm, 7 mm s^{-1} and 0.184 g s^{-1} Ni and 0.074 g s^{-1} Al, (a) transverse section – optical micrograph; (b) EDS analysis across the transverse section from the substrate/clad interface to the top surface; 0 at % Al; ● at % Cr, (c) transverse section – SEM micrograph showing cellular/dendritic structure in region of dilution; (d) TEM micrograph from the lower part of the clad layer, i.e. dilution region; and (e) TEM micrograph from the main region of clad layer. See Table II for compositions at positions A, B, C, and D in (d) and (e).

compositional analysis. Thin foils were prepared from selected layers using an electropolishing solution consisting of 60 ml perchloric acid, 350 ml *n*-butanol, and 590 ml methanol. Optical microscopy, scanning electron microscopy (SEM) together with energy dispersive spectrometry (EDS), transmission electron microscopy (TEM) and scanning transmission electron microscopy (STEM) were used to determine the microstructural and compositional characteristics.

3. Results and discussion

3.1. Single layers Ni–Al based

Fig. 1(a) shows a transverse section of a Ni–Al clad layer produced at 1.8 kW, 3 mm, 7 mm s^{-1},

TABLE I Dimensions and compositions (at %) of Ni–Al single clad layers

Sample	Powder flow rate ($g s^{-1}$)		Dimensions (mm)		% Dilution	Calculated composition		EDS analysis (at %)				
	Nickel	Aluminium	Width	Thickness		(a)	(b)	Ni	Al	Cr	Co	Mo
1	0.184	0.040	3.0	1.06	~ 18	32	26	Balance	28	5	1.5	1
2	0.184	0.074	2.70	1.54	~ 10	46	41	Balance	36.5	3.5	2.0	0.4
3	0.184	0.100	2.50	1.84	~ 2	54	53	Balance	54	0.4	–	–

[a] Composition estimated from feed rate.
[b] Composition estimated from the feed rate with dilution taken into acount and assuming uniform composition across the whole processed zone.

$0.184\ g s^{-1}$ Ni powder flow rate and $0.074\ g s^{-1}$ Al powder flow rate. Columnar grains of ~0.2 mm width are seen. EDS analysis data on a line from the interface between the processed zone and the substrate to the top of the clad layer are shown in Fig. 1(b). The major part of the clad layer above the original level of the substrate surface showed reasonable homogeneity of composition: Al ~ 36.5 ± 2 at % and Cr ~ 3.5 ± 1 at % (Table I, sample 2). The presence of Cr derives from the dilution effect from the melted region of the substrate (other elements from the substrate, such as Mo and Co, were also present in small amounts but are not shown in Fig. 1(b)). The main dilution effect was located in the region below, and extending to a little above, the original level of the substrate surface. In this region there was a substantial compositional gradient; the Al content was lower and the Cr content was higher than in the upper, main part of the clad. Fig. 1(c) shows the cellular/dendritic structure in this region of dilution. The dilution was calculated from the ratio of the area of clad below the original level of the substrate to that above as measured from transverse sections. Dilution values varied by about 20% along a clad layer; therefore the values quoted in Table I must be viewed as approximate. The observations show that the laser processing conditions employed led to good mixing throughout the clad except in the interface region. The average Al content of the powder feed mixture (as calculated from the relative flow rates of nickel and aluminium) was ~46 at %. However, taking into account the dilution effect from the substrate (estimated as a dilution of ~10 vol %) reduces the estimated value to ~41%. Although this estimated value is higher than the EDS analysis, if the estimated and EDS values for the other processing conditions are also considered (Table I) it appears that there is no significant loss of Al during laser processing.

TEM using selected area diffraction pattern (SADP) and STEM (Table II) investigation of an area near the substrate interface (Fig. 1(d), region A) showed cells/dendrites containing 25 at % Al and 6 at % Cr; these are considered to be Ni_3Al (γ') with Cr in solid solution [4]. The regions between the cells/dendrites (region B) containing 11 at % Al and 17 at % Cr, together with substantial amounts of Co and Mo, are interpreted as Ni-based solid solution (γ). In the main part of the clad (Fig. 1(e)) the cells/dendrites (region C) contain 33 at % Al, consistent with NiAl intermetallic compound (β) with a small amount of Cr and other

TABLE II STEM analysis of the single clad layer (sample 2)

Feature	Composition (at %)				
	Ni	Al	Cr	Co	Mo
A	Balance	25	6	2	1
B	Balance	11	17	8	6
C	Balance	33	2.5	1.4	0.25
D	Balance	–	24	3.6	34

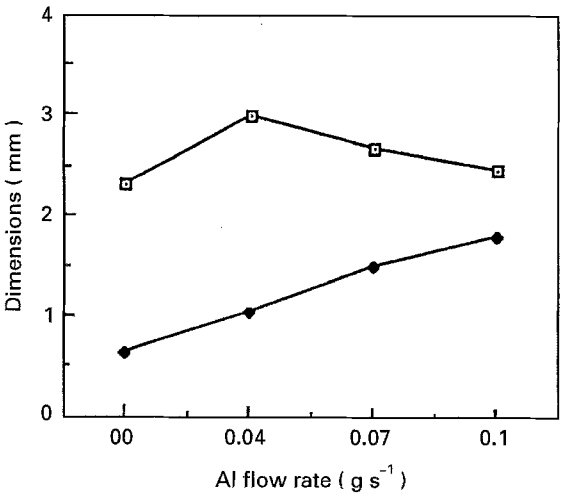

Figure 2 Effect of Al powder flow rate on the dimensions of Ni–Al single clad layers processed at 1.8 kW, 3 mm, $7\ mm\ s^{-1}$ and $0.184\ g s^{-1}$ Ni flow rate (note thickness = distance from the substrate/clad interface to the top of the clad). ⊡ width; ◆ thickness.

elements in solid solution. The regions between the cells/dendrites (region D), which occupy only a small volume fraction of the clad, contain virtually no Al but consist of ~42 at % (Ni + Co), 24 at % Cr and 34 at % Mo. It is not clear whether these regions consist only of a single phase or whether they contain particles in a matrix phase. Reference to the Ni–Cr–Mo phase diagram [5] leads to the suggestion that these regions consist predominantly of one of the ternary compounds based on this system, possibly P phase, which may have formed as a constituent of a eutectic reaction.

Table I and Fig. 2 show the effect of increasing Al powder flow rate from 0.040 to $0.100\ g s^{-1}$ while keeping the Ni powder flow rate constant at $0.184\ g s^{-1}$ for

a series of a single clad layers; Fig. 2 includes the dimensions of a layer produced using only Ni powder. All the clad layers exhibited a limited amount of transverse cracking but longitudinal cracks were not observed. EDS analysis showed that in each of the clad layers the Al content in the upper (main) region was reasonably uniform as shown in Fig. 1 for Al powder flow rate of 0.074 $g\,s^{-1}$. The change in the compositions and dimensions with increasing Al feed rate can be summarized as follows: (i) there was an approximately linear increase in Al content in the upper region of the clad (Table I) (ii) the clad width varied only slightly whereas the clad thickness increased continuously (Fig. 2).

The structures of samples 1 and 3 were not investigated in detail, but from phase diagram considerations [4], sample 1 containing 28 at % Al is expected to consist mainly of γ', with a small proportion of β phase, while sample 3, containing 54 at % Al should consist essentially of β phase.

3.2. Functionally graded clads Ni–Al based

Fig. 3 (a–c) show single, double and triple layer coatings on a Ni alloy substrate and their compositions are shown in Table III. The interfaces between each layer were curved, and columnar growth occurred from the base to the top of the sequence of layers; heat flow appears to be predominantly directional from the clad into the substrate although there was some evidence of an equiaxed zone at the top of the FGMs. SEM examination of the first layer of the FGMs showed a cellular/dendritic structure as illustrated in Fig. 3(d) for the double layer sample. SEM–EDS analysis (Table III) taken from the mid-position of layer 1 of the FG coatings shows the presence of 29–30 at % Al; STEM data for layer 1 of the double layer FG coating (Table IV) show that the cells/dendrites (region A, Fig. 3(e)) contain 31 at % Al, which is consistent with NiAl (β phase) and is in agreement with the composition of region C in Table II; selected area diffraction analysis confirmed the B2

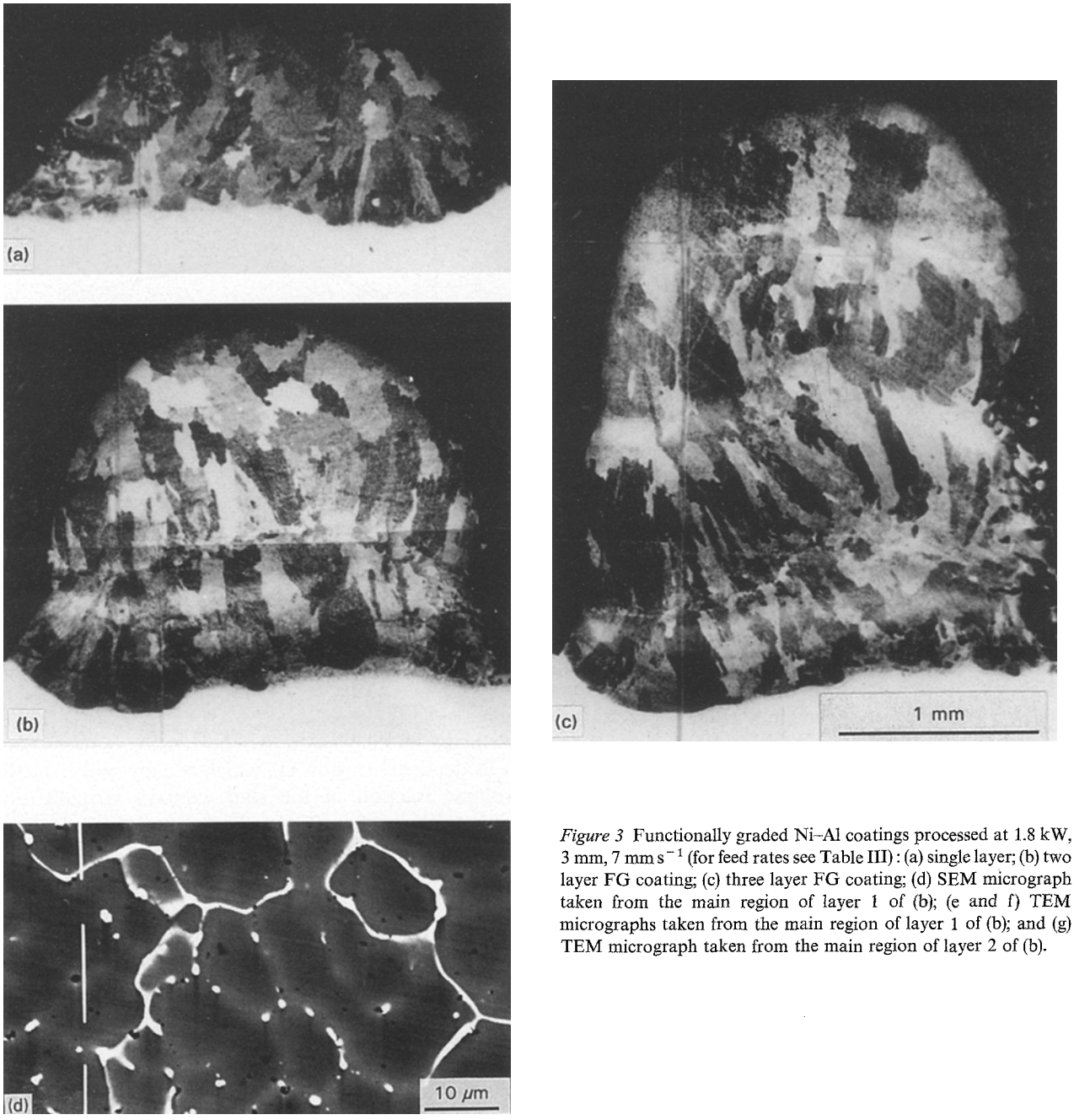

Figure 3 Functionally graded Ni–Al coatings processed at 1.8 kW, 3 mm, 7 mm s^{-1} (for feed rates see Table III): (a) single layer; (b) two layer FG coating; (c) three layer FG coating; (d) SEM micrograph taken from the main region of layer 1 of (b); (e and f) TEM micrographs taken from the main region of layer 1 of (b); and (g) TEM micrograph taken from the main region of layer 2 of (b).

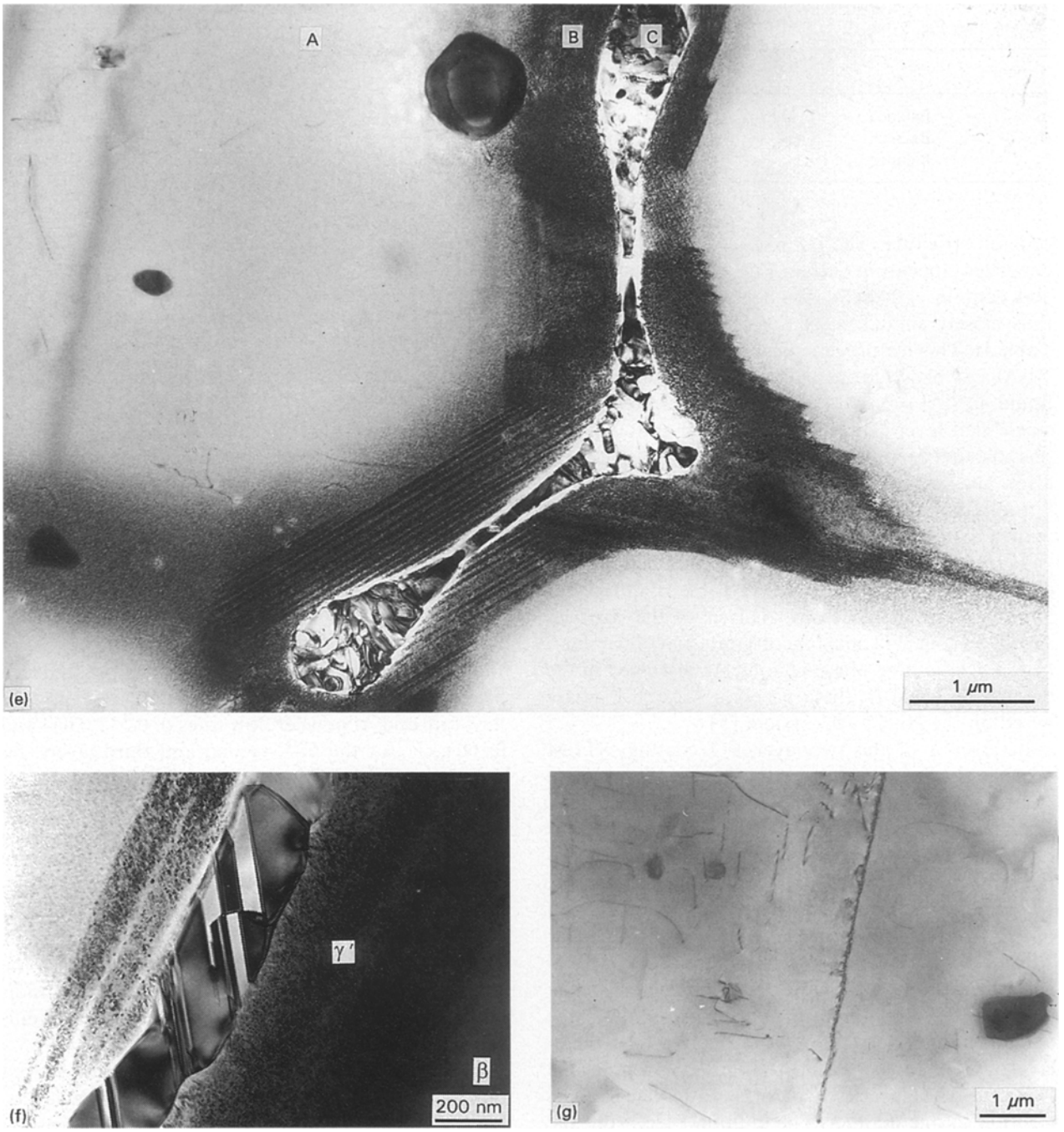

Figure 3 Continued.

TABLE III Data for FGM of Ni–Al clad layers superimposed on Ni alloy substrate

Clad	Powder flow rate ($g\,s^{-1}$)		EDS analysis (at %)				
	Nickel	Aluminium	Ni	Al	Cr	Co	Mo
Single	0.183	0.033	Balance	28	3	1.3	1.5
Two layers							
Layer 1	0.183	0.033	Balance	29	2.3	2.0	1.4
Layer 2	0.183	0.057	Balance	39	2.0	2.7	1.2
Three layers							
Layer 1	0.183	0.033	Balance	30	2.4	2	1.0
Layer 2	0.183	0.057	Balance	40	1.4	0.5	0.4
Layer 3	0.183	0.085	Balance	56	0.5	–	–

TABLE IV STEM analysis (at %) of layer 1 of two layer FG coating – see Fig. 3 (b)

Region	Ni	Al	Cr	Co	Mo
A	Balance	31	3	1.5	0.25
B	Balance	24	6	2.2	1.8
C	Balance	–	24	5	35

ordered structure. The peripheries (B) of NiAl cells/dendrites (appearing dark in Fig. 3(e)) show striations and contain ~24 at % Al and 6 at % Cr and were thus closely similar in composition to region A in Table II. This feature is interpreted as being a rim of Ni_3Al (γ') phase formed by the peritectic reaction: liquid + NiAl ⇒ Ni_3Al (this was not detected in the single clad layer (Table I and Fig. 1(d) although it is possible that a similar, narrow layer was present there also). The intercellular/interdendritic regions (C) have virtually no Al content but show particles (Fig. 3(f)) with a banded substructure and containing (at %) ~41 (Ni + Co), 24 Cr; 35 Mo; this composition is in close agreement with region D in Table II although it is possible that the STEM analysis of the particles shown in Fig. 3(f) may incorporate a contribution from the adjoining phase regions. As discussed in the context of Table II, these particles may be P phase based on the Ni–Cr–Mo system [5].

In layer 2 of the two-layer FG coating, STEM analysis showed the structure to be essentially single phase, with an Al content between 38 and 41 and Cr 1.5 at %, corresponding to the NiAl phase; this is consistent with phase diagram considerations. Also present are a few small particles rich in Al and Ni, whose origin is not known (Fig. 3(g)). Layers 2 and 3 of the three-layer FG coating were not examined by TEM.

The composition of the single layer sample in Table III is in reasonable agreement, as expected, with the compositions of the first layer of the two- and three-layer FG coatings. Also the second layers in the two- and three-layer FG coatings are similar in composition to one another. The dilution effect from the substrate is expected to diminish in successively superimposed layers, i.e. the content of chromium, etc. should decrease. This effect is clearly shown in the top layer of the three-layer sample, and also, although less clearly, in the second layers of the FG coatings.

3.3. Single layers: Fe–Al

A series of crack free single Fe–Al clad layers were produced using the same two feeder technique as for Ni–Al i.e. by blowing Fe powder (flow rate 0.154 $g s^{-1}$) and Al powder (flow rates in the range 0.044 to 0.100 $g s^{-1}$) into the laser melted zone of a low carbon steel substrate and employing the same laser processing parameters as used for the Ni–Al system. Optical and SEM examination of sample 2, which was produced with the mid-range Al powder feed rate (0.074 $g s^{-1}$), revealed a columnar grain structure. TEM observations showed the microstructure to be single phase and SEM-EDS analysis (Table V) gave an

TABLE V Data for Fe–Al single clad layers and FG coatings

Sample	Flow rate (Fe $g s^{-1}$	Flow rate (Al) $g s^{-1}$	Composition, at % Al		
			SEM–EDS	Calculated (a)	(b)
Single-1	0.154	0.044	30	37[a]	30[b]
Single-2	0.154	0.074	42	50	45
Single-3	0.154	0.100	52	57	56
FGM-1	0.183	0.032	22		
FGM-2	0.183	0.064	29		
FGM-3	0.183	0.100	37		

[a] Composition estimated from feed rate.
[b] Composition estimated from the feed rate with dilution taken into account and assuming uniform composition across the whole processed zone

Al content of ~42 at % which is consistent with the ordered α_2-phase of the Fe–Al system [6]. Table V also demonstrates that, as found for the Ni–Al single clads, the composition may be estimated from the feed rates and that there is no evidence for a significant loss of Al during processing.

3.4. Functionally graded layers: Fe–Al

FG Fe–Al coatings were produced using the standard processing parameters with 0.183 $g s^{-1}$ Fe powder flow rate and Al powder flow rates of 0.032, 0.064 and 0.100 $g s^{-1}$ for the first, second and third layers, respectively. SEM–EDS area analysis (10 × 5 μm) gave average values of 22, 29 and 37 at % Al in the first, second and third layers, respectively (Table V). The Al content near the interface between layers was less than the average composition of the upper, higher Al content layer due to dilution. Columnar grains grew epitaxially at the interfaces between clad layers (Fig. 4). The presence of equiaxed crystals at the top of the third layer suggest significant heat transfer by radiation and convection in the final stage of solidification. No cracks were observed.

The thickness of the layers increased with Al feed rate showing the same trend as for the Ni based layers. However the third layer also exhibited an increase in width associated with spherical type geometry (Fig. 4) not seen in the Ni based layers. The shape is considered to be sensitive to the surface tension and viscosity of the melt. The Al content in single and FG coatings for both the Ni–Al and Fe–Al systems increased with increasing Al powder flow rate (Fig. 5). For the production of single layers the Fe flow rate was nearly 20% less than the Ni flow rate. These flow rates gave single layers of approximately the same Al content in at % for a given Al flow rate (calculations, without correcting for dilution, of the Al contents show a difference of only ~1 at % at Al flow rate of 0.04 $g s^{-1}$ and ~3 at % at 0.100 $g s^{-1}$ with the smaller value for Ni–Al system in each case). It can be seen that the best fit linear plots to the single layer data almost superimpose for the Ni–Al and the Fe–Al systems as predicted from the flow rates, i.e. for these systems the composition is determined by the flow rates and the characteristics of the elemental constituents involved have negligible effect. The Ni

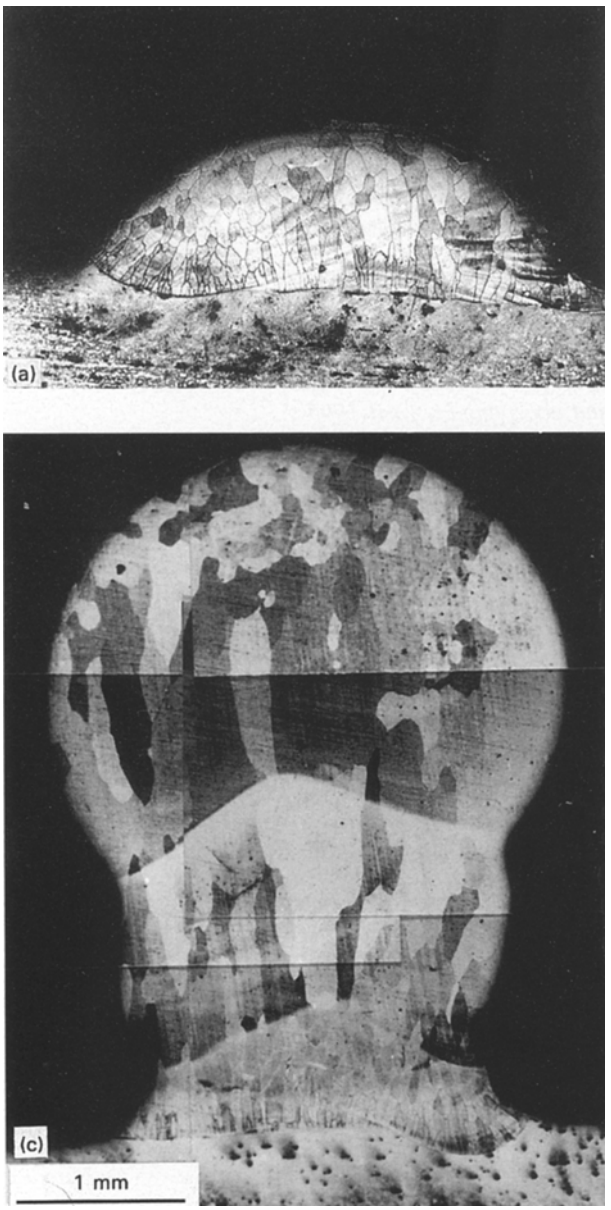

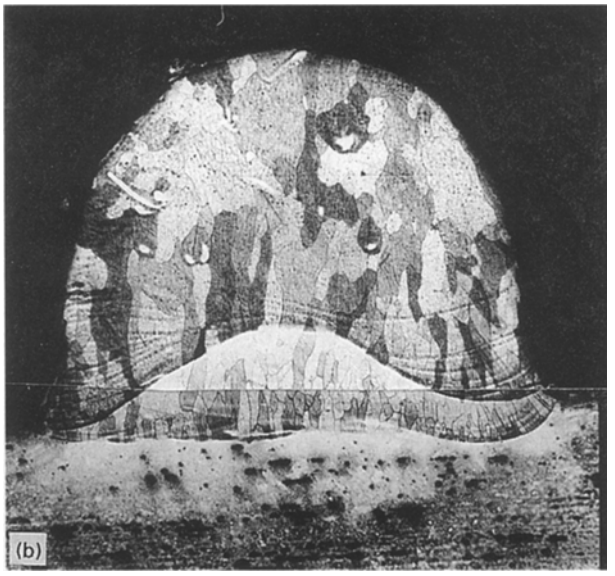

Figure 4 Optical macrographs of transverse sections of functionally graded Fe–Al coatings produced at 1.8 kW, 3 mm, 7 mm s^{-1} and 0.183 g s^{-1} Fe and various Al powder flow rates (0.032 to 0.1 g s^{-1}); (a) single layer; (b) two-layer FG coating; (c) three-layer FG coatings.

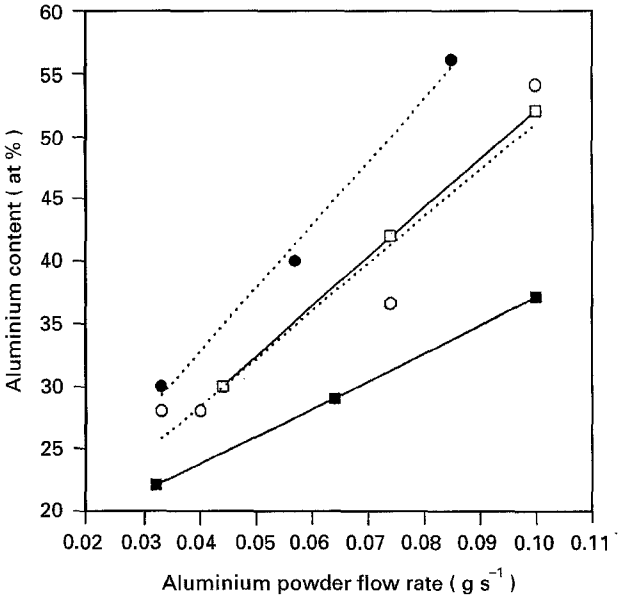

Figure 5 Variation of average Al content with Al powder flow rates for single and FG coatings of Ni–Al and Fe–Al (Ni and Fe powder feed rates were 0.183 ± 0, 001 g s^{-1} except for the single layer Fe–Al coatings where 0.154 g s^{-1} was used: laser parameters 1.8 kW, 3 mm, 7 mm s^{-1}). □ Fe–Al single layer; ■ Fe–Al FG coating; ○ Ni–Al single layer; ● Ni–Al FG coating.

flow rate used for the FG Ni–Al coatings was the same (0.183 ± 0.001 g s^{-1}) as for the production of the single Ni–Al coatings and hence the composition of the first layer lies close to the experimental value for the corresponding single layer. However, the second and third layers of the FG coatings have Al contents in excess of those that would be obtained from a single layer under the same processing conditions. This is due to the nickel entering the layers through dilution being less for the second and third layers of the FG coatings; dilution in the case of the single layers and the first layer of the FG coatings is from a high Ni content alloy whereas for the second and third layers dilution is from a lower Ni content alloy. It must be emphasized that there is control of the composition of the layers of the FG coatings through adjustment of the flow rates. For example the Fe flow rate of 0.183 g s^{-1} used for the Fe–Al FG coatings was greater than that used for the single layers and hence it is expected that the Al content for a given Al flow rate is less for the FG coating; this is confirmed in Fig. 5 where it can be seen that the compositional data for all the layers of the FG coating lie below the curve for the single layers.

4. Summary and conclusions

1. Single clad layers based on nickel–aluminides and iron–aluminides can be produced on nickel and iron based substrates, respectively, by a laser process utilizing two powder feeders to supply the required combinations of elemental constituents: nickel and aluminium or iron and aluminium. *In-situ* alloying occurs in the laser generated melt pool and compositional control is exercised via the powder feeder rates.

The composition of the layers may be estimated from the feed rates.

2. Functionally graded coatings (up to several mm in total height) can be produced by superimposition of a series of layers of different compositions. As for the single layers, it has been demonstrated that adjustment of the feed rates allows control of the composition of the different layers in a functionally graded coating.

Acknowledgements

Acknowledgements are made to SERC for financial support and to INCO Alloys for supplying the nickel alloy substrate material.

References

1. J. H. ABBOUD, D. R. F. WEST and R. D. RAWLINGS, *Mater. Sci. Technol.* **10** (1994) 414.
2. *Idem., J. Mater. Sci.* **29** (1994) 3393.
3. K. MOHAMMED JASIM, R. D. RAWLINGS and D. R. F. WEST, *J. Mater. Sci.* **28** (1993) 2820.
4. A. TAYLOR and R.W. FLOYD, *J. Inst. Met.* **81** (1952–3) 451.
5. A. K. JENA, S. B. RAJENDRAPRASAD and K. P. GUPTA, *J. Alloy Phase Diagrams, Indian Institute of Metals* **5** (1989) 164.
6. Binary Alloy Phase Diagrams, vol. 1, Editor in Chief. T. B. Massalski (ASM, Ohio, 1986) p. 111 and 112.

Received 21 March
and accepted 11 April 1995